ACS APPLIED MATERIALS & INTERFACES

Research Article

www.acsami.org

Formation and Mechanical Characterization of Aminoplast Core/Shell Microcapsules

Melanie Pretzl,[†] Martin Neubauer,[†] Melanie Tekaat,[†] Carmen Kunert,[†] Christian Kuttner,[†] Géraldine Leon,[‡] Damien Berthier,[‡] Philipp Erni,[‡] Lahoussine Ouali,[‡] and Andreas Fery*[,†]

[†]Department of Physical Chemistry II, University of Bayreuth, Universitätsstraße 30, D-95447 Bayreuth, Germany

[‡]Firmenich SA, Cooperate R&D Division, P.O. Box 239, CH-1211 Geneva 8, Switzerland

Supporting Information

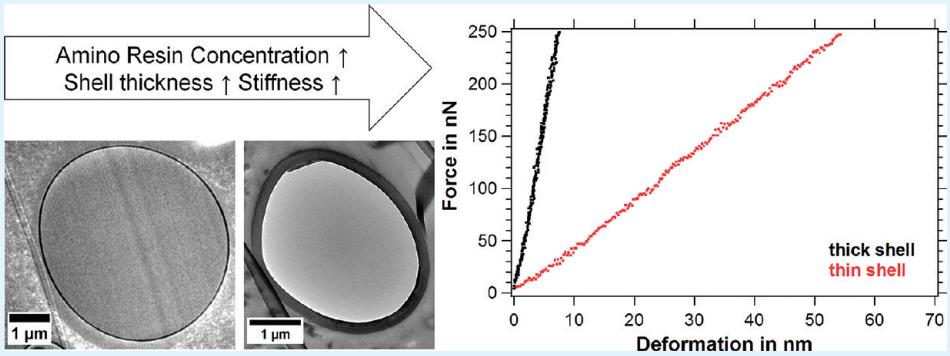

ABSTRACT: This work aims at establishing a link between process conditions and resulting micromechanical properties for aminoplast core/shell microcapsules. The investigated capsules were produced by the in situ polymerization of melamine formaldehyde resins, which represents a widely used and industrially relevant approach in the field of microencapsulation. Within our study, we present a quantitative morphological analysis of the capsules' size and shell thickness. The diameter of the investigated capsules ranged from 10 to 50 μm and the shell thickness was found in a range between 50 and 200 nm. As key parameter for the control of the shell thickness, we identified the amount of amino resin per total surface area of the dispersed phase. Mechanical properties were investigated using small deformations on the order of the shell thickness by atomic force microscopy with a colloidal probe setup. The obtained capsule stiffness increased with an increasing shell thickness from 2 to 30 N/m and thus showed the same trend on the process parameters as the shell thickness. A simple analytical model was adopted to explain the relation between capsules' geometry and mechanics and to estimate the elastic modulus of the shell about 1.7 GPa. Thus, this work provides strategies for a rational design of microcapsule mechanics.

KEYWORDS: *hollow polymer shells, melamine formaldehyde capsules, compression behavior, stability, elastic properties, controlled release, emulsions*

INTRODUCTION

Microcapsules are of broad interest not only in fundamental science[1,2] but also in a wide range of applications. Whenever the functionality of an active substance needs to be protected and/or a controlled release is demanded, microencapsulation is a frequently used solution.[3−10] Industrially relevant wall materials are amino resins, like melamine formaldehyde (MF), because this class of resins is produced from cheap raw materials, widely applicable, and economical to use.[10] In particular, aminoplast core/shell microcapsules are suitable for the encapsulation of pressure sensitive recording materials,[10] perfume fragrances,[11,12] phase change materials,[13,14] self-healing composites,[15,16] agrochemicals,[17] or analytes in biosensor applications.[18] All these applications require a particular mechanical stability, compliance, release, shelf life, and adhesion of the microcapsules.[19,20] Therefore, a rational process design of microcapsules is desired to individually tailor their mechanical properties.[21] To establish correlations between process parameters and the resulting capsule mechanics, methods are favored that allow an investigation of microcapsule mechanics on the single-particle level.[20]

So far, reported mechanical characterizations on aminoplast microcapsules were focused on compression experiments with the single capsule compression apparatus described by Keller and Sottos[22] and the micromanipulation technique described by Zhang and co-workers.[23] With both setups, individual microcapsules were deformed in the range of micrometers under applied force loads of millinewtons. Thus, the authors were able to access a deformation regime where rupture forces and the failure of microcapsules can be successfully

Received: February 16, 2012
Accepted: May 14, 2012
Published: May 14, 2012

determined.[24−28] To understand how our approach differs from the ones used in previous studies, the definition of the terms "small deformation" and "large deformation" is crucial. In general, the mechanical response of a material can be elastic or plastic. In brief, an elastic response is characterized by a full recovery of the material's original shape, whereas a plastic response is accompanied by a permanent change of the material's shape (e.g., buckling or capsule failure). In material sciences, small deformations are often referred to compression tests carried out in the elastic regime. We stress that for our approach, the critical parameter used for the definition of small and large deformations is the microcapsule's shell thickness and not the yield point, which describes the transition between the elastic and plastic regime. Hence, small deformations are understood in this publication as compressions below or on the order of the shell thickness and large deformations as compressions larger than the shell thickness. There is one pioneering paper by Mercadé-Prieto[29] where finite element modeling has been used to estimate the wall thickness to radius ratio and the elastic modulus of individual capsules from compression experiments in the elastic regime. We appreciate the approach of the authors because it offers the possibility to estimate the critical mechanical parameters for individual capsules. However, for this publication, the included experimental data concentrates on fractional deformations between small deformations on the order of the shell thickness and very high deformations.[29] In contrast to previous studies, our interest is concentrated on the mechanical response of capsules in the small deformation regime, which refers to a compression of the capsule on the order of the shell thickness. This regime has not yet been explored for aminoplast microcapsules, which is unfortunate, because it offers the possibility to link the capsules' mechanical response to its geometric design. For polyelectrolyte multilayer capsules it has been shown[30] that this regime is also relevant for adhesion properties. Atomic force microscopy (AFM) is an ideal tool to carry out deformations of capsules on the order of the shell thickness, because it offers a displacement resolution of nanometers and a force resolution of piconewtons. The compression apparatuses used in previous studies show with a resolution of a few hundred nanonewtons a sufficient resolution to investigate the elastic response of many capsule systems. Indeed the limiting factor for small deformation experiments is also often not the force resolution but the resolution of the induced deformation.

Several strategies exist for the synthesis of aminoplast core/shell microcapsules,[10,31] but the most applied and industrially relevant is the in situ polymerization,[32,33] which sometimes is also referred to as phase separation method.[12] In this emulsion-templated process, the hydrophobic core material is dispersed in form of small oil droplets in the aqueous continuous phase, where the MF prepolymer is dissolved. The polycondensation of the prepolymers starts under acidic conditions and elevated temperatures. Formed oligomers are deposited at the oil/water interface, where they polymerize to a three-dimensional shell around the oil droplet.[13,34] To control capsule mechanics process parameters are interesting that affect size, shell thickness and the elastic modulus of the wall material. Typically, a polydispersity in size is observed for capsules manufactured with the in situ polymerization. These size distributions are determined by the produced emulsion droplets, which serve as soft templates for the buildup of the shell. Key parameters for the adjustment of the emulsion droplet size are the interfacial tension between core and continuous phase and the energy dissipation of the stirrer.[13,27] In general, the in situ polymerization yields aminoplast core/shell microcapsules between 5 and 50 μm,[32] where smaller capsules show narrower size distributions than larger capsules.[35] The shell thickness is expected to be between 30 and 300 nm[32] and can be adjusted by the ratio of melamine to formaldehyde,[12] the reaction time,[24] pH,[34] and the core to shell mass ratio per created surface area of the emulsion droplets.[13] The elastic modulus of the shell depends on the used wall material[36] and can be changed through chemical modifications and/or the cross-linking density.

In this paper, we investigate aminoplast core/shell microcapsules and strategies to rationally design their mechanical properties. The motivation to focus on aminoplast microcapsules is based on their regular application in different industrial fields.[5,11] Challenging for the presented work was the polydispersity of the studied capsules that is very well reflecting the actual industrial situation for amino resin microcapsules produced by an emulsion-templated in situ polymerization. Structure property relations are often not efficiently resolved by standard methods employed during industrial quality assurance. Therefore, the characterization on the single particle level is crucial for such size-dispersed systems. For this reason, we have chosen methods that are able to resolve and quantify the geometry and mechanics of single microcapsules. In particular, we used transmission electron microscopy (TEM) to determine the shell thickness from ultrathin sections of Epon-embedded microcapsules. With AFM and a colloidal probe setup we studied the mechanical response of single capsules in the small deformation regime, which refers to a capsule compressions on the order of the shell thickness. Subsequently, we correlated the obtained shell thickness with the process parameters and then via a simple analytical model with the resulting capsule mechanics. The full correlation between process parameters and resulting mechanical properties suggests strategies to rationally tailor microcapsules produced by an industrial relevant process.

EXPERIMENTAL SECTION

Materials. The key ingredients for the microcapsules synthesis are the melamine-formaldehyde resin (Urecoll SMV, BASF); a colloidal stabilizer (Poly(acrylamide 20%, acrylic acid 80%) sodium salt, Sigma Aldrich); a formaldehyde scavenger (ethylene urea, Fluka); acetic acid and sodium hydroxide for pH adjustments. The core liquid is a mixture of a 5-'model' fragrance compound, as described previously:[5] hexyl salicylate 20% w/w, (+-)-methyl 2,2-dimethyl-6-methylene-1-cyclohexanecarboxylate 20% w/w (Romascone), 3-(4-tert-butylphenyl)-2-methylpropanal 20% w/w (Lilial), cis/trans-4-tert-butyl-1-cyclohexyl acetate 20% w/w (Vertenex), and (+-)-2-tert-butyl-1-cyclohexyl acetate 20% w/w) (Verdox). As dispersant, we used demineralized water.

Synthesis of Microcapsules. Standard core/shell capsules were synthesized according to protocols described previously.[12,32,33] The specified amounts of the resin, colloidal stabilizer, and water were introduced into a 250 mL reactor at room temperature (pH 7.50). The reaction mixture was sheared at 800 rpm with an anchor stirrer. A resin to oil mass ratio of 0.149 g/g was chosen for the standard core/shell capsules. Then acetic acid (0.78 g) was added for the adjustment of the pH (pH 5.14). The perfume oil (95.00 g) containing Rhodamine (0.1% w/w, Fluka) was added, and the reaction mixture was warmed up to 40 °C and stirred for 1 h. Afterward the reaction mixture was stirred at 55 °C for 3 h. Finally, ethylene urea (50% in water w/w, 16.00 g) was added, and the reaction mixture was stirred at 60 °C for 1 h. Then, the mixture was cooled to room temperature (pH 5.65) and

Table 1. Microcapsules Prepared with Different Amounts of Resin and the Obtained Results from the Morphological and Mechanical Characterization: Average Diameter d, Zeta Potential ζ, Measured Shell Thickness h_i, Correction Factor f, Corrected Shell Thickness h, and Capsule Stiffness F/D

amino resin (%)	perfume (%)	d (μm)	ζ (mV)	h_i (nm)[a]	f	h (nm)	F/D (N/m)[a]
100	43.5	34	−48	285 ± 71	0.64	182	29 ± 11
100	45.3	31	−50	214 ± 61	0.57	122	19 ± 7
75	43.5	18	−48	122 ± 16	0.63	77	5.2 ± 2.0
50	44.8	28	−46	103 ± 38	0.63	65	1.7 ± 3
50	46.4	28	−56	103 ± 38	0.63	65	1.7 ± 3
25	47.9	43	−28				

[a]The standard deviation σ of the thickness and stiffness distributions refers to the fit coefficient width w by the following relation $\sigma = w/(2^{1/2})$.

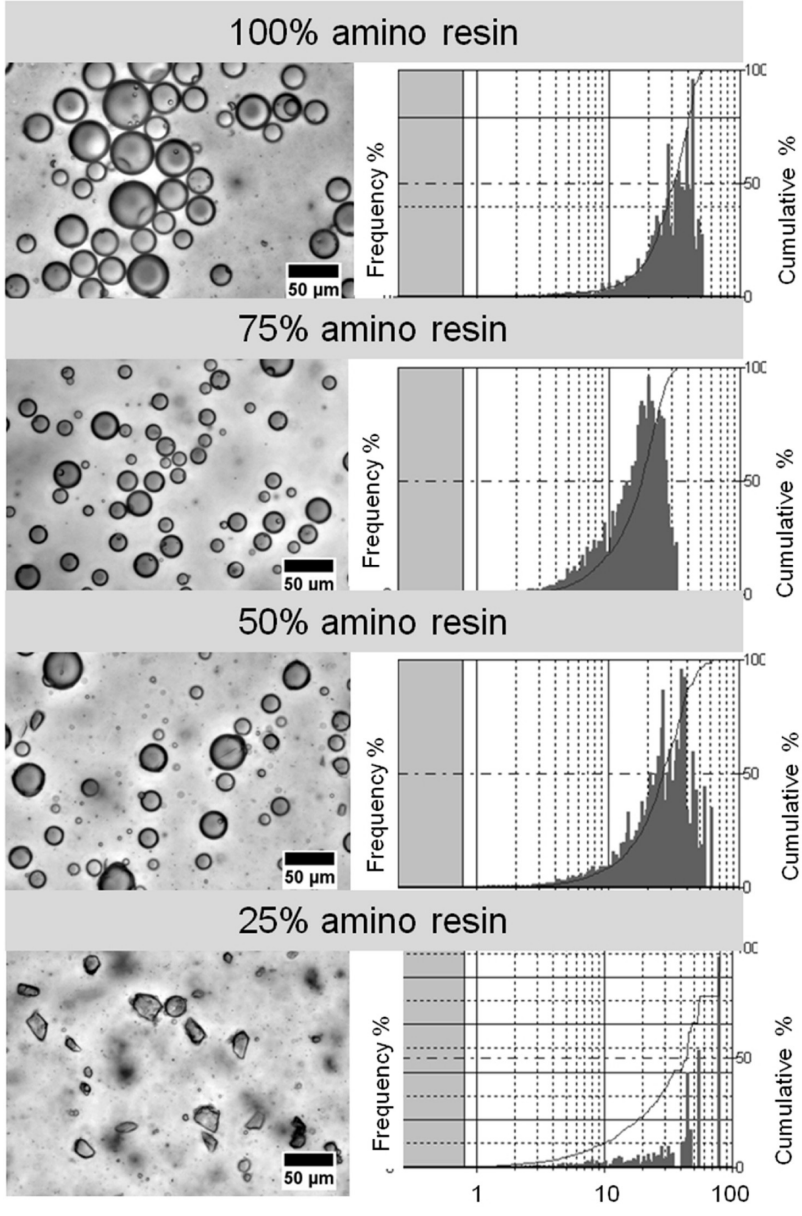

Figure 1. Optical micrographs and size distributions of the produced aminoplast core/shell microcapsules. For a 25% level of amino resin, the encapsulation process failed and microcapsules with a deformed capsule shape were produced that were not able to form a stable shell around the dispersed oil droplets.

neutralized with NaOH (30% in water w/w, 0.92 g) to give a final pH of 6.57 in the aqueous dispersion.

Morphological Characterization. Size distributions were determined with a flow particle image analyzer FPIA (Sysmex FPIA-300, Malvern Instruments). Zeta potential measurements (Zetasizer, Malvern) of the diluted capsule slurries yielded negative values, which typically range from −30 to −50 mV (see Table 1). With TEM (Zeiss CEM 902) thin sections of about 50 to 60 nm, produced by an ultracut microtome (Leica EM UC7), were imaged at 80 eV. The shell thickness was obtained from TEM images by extracting cross-sectional

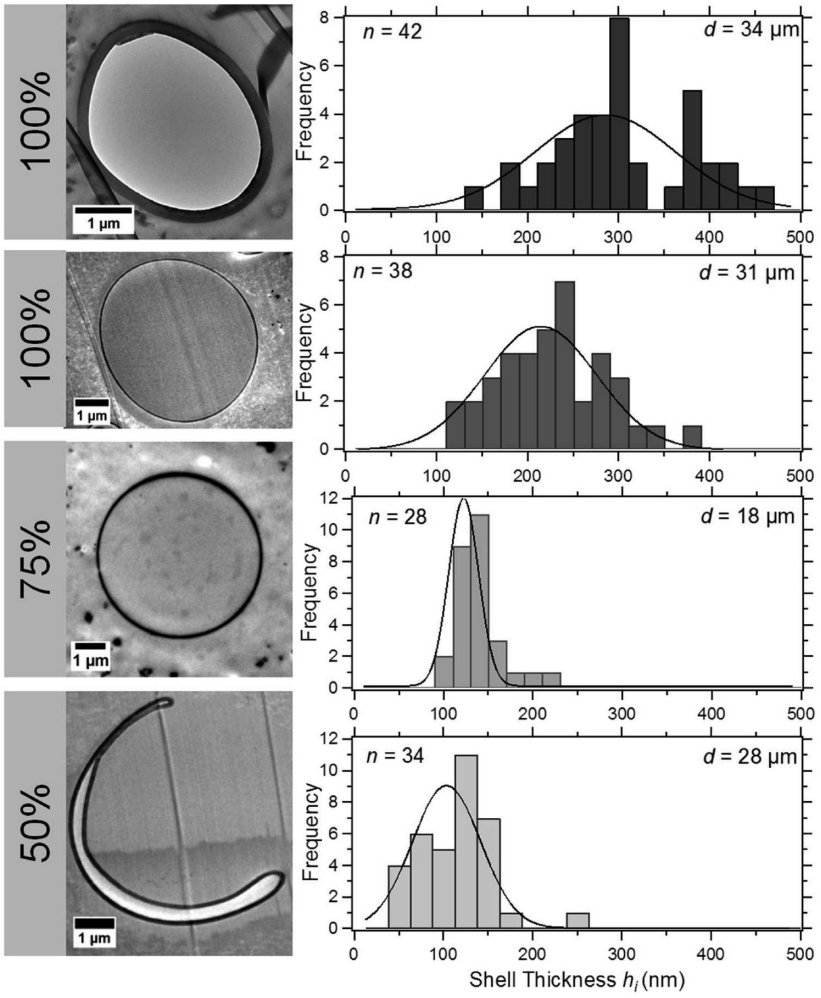

Figure 2. TEM images of embedded microcapsules sectioned with an ultra microtome and the quantified distribution of the measured shell thickness. The number of analyzed sections n is indicated along with the used amount of resin in percentage and the average diameter d.

gray value profiles that were analyzed with ImageJ software. The start/end of the shell was determined at 50% decrease/increase of the gray value intensity. TEM samples were prepared by mixing the capsule solution in a 1:1 ratio with 2% aqueous solution of agar (Agar Noble, Difco). After curing, the flexible gel was cut with a scalpel into small cubes. Next, the agar-embedded capsules were solidified by 1 h incubation with a 2% glutaraldehyde solution (Serva Electrophoresis GmbH) in phosphate buffer (0.05 M Phophate Buffer, pH 7.4 Merck). Afterward three washing steps with phosphate buffer (0.05 M, pH 7.4, Merck) were used to remove the excess of glutaraldehyde. Then the samples were dehydrated in ethanol−water mixtures with increasing ethanol content (30%/50%/70%/95%) and three times to pure ethanol (VWR International). The dehydration exposure time was 15 min for each step. Then the dried samples were mixed with Epon 812 (Serva Electrophoresis GmbH): Epon 812/ethanol mixture (1:1) for 12 h, followed by an Epon 812/ethanol mixture (3:1) for 3−4 h and finished with three immersion steps (3−4 h) in 100% Epon 812.

Mechanical Characterization. Force spectroscopy experiments were performed in aqueous environment with a commercial AFM setup: Nanowizard (JPK Instruments, Germany) combined with an inverted optical microscope Axiovert 200 (Zeiss, Germany). The optical microscope was used to determine the size of the microcapsule before the deformation experiment and to align the cantilever probe with the center of the immobilized microcapsule. During the capsules' compression we used the microinterferometry[37] mode of the microscope to follow in situ the change of the apparent contact area between microcapsule and substrate. Only elastic and uniform capsule deformations were used for evaluation. The deformations were performed using the colloidal probe technique,[38,39] in which silica particles (diameter 30−40 μm; Polysciences Inc., USA) were attached to tipless silicon cantilevers (ACT-TL, k_c = 25−75 N/m, f_c = 200−400 kHz, AppNano). The colloids were attached using a micromanipulator (MP-285; Sutter Instruments) and two-component epoxy glue (UHU Plus Endfest 300, UHU GmbH & Co. KG, Germany). After attachment, the colloidal probe cantilevers were cleaned by exposure to atmospheric plasma (5 min, high intensity, Plasma Technology). Spring constants of the cantilevers were determined with the thermal noise method,[40,41] which is implemented in the commercial JPK software. Only cantilevers were used that were in accordance with the frequency and spring constant range reported by the manufacturer. The experiments in aqueous solution were carried out in liquid cells, made of a plastic ring (diameter 24 mm, height 5 mm) and a coverslip (diameter 24 mm, thickness 0.13−0.16 mm, Menzel). The liquid cells were cleaned with an isopropanol/ethanol/water mixture (1:1:1) and through exposure to an atmospheric plasma (5 min, high intensity, Plasma Technology). To keep the negatively charged microcapsules immobilized in the liquid cell we used branched polyethyleneimine (PEI, M_w 25.000 g/mol, 1 g/L aqueous solution, Sigma Aldrich) as surface coating. To obtain individual and separated microcapsules for force spectroscopy experiments and to remove nonimmobilized capsules the sample was washed several times with purified water (Millipore Advantage) in the liquid cell. Reference curves on hard substrates were obtained before and after each capsule deformation to ensure a constant optical lever sensitivity, which is necessary for reliable and comparable force deformation curves.[42]

RESULT AND DISCUSSION

Morphology of Aminoplast Core/Shell Microcapsules.

Size, shell thickness and the used wall material are important parameters for the mechanics of microcapsules. A possible parameter to adjust the shell thickness of aminoplast microcapsules is the resin concentration.[13] For the microcapsules production the fragrance oil is dispersed by emulsification in the continuous aqueous phase. The melamine formaldehyde prepolymer, which is dissolved in the continuous phase, will start to form oligomers under acidic conditions and elevated temperatures. These oligomers then deposit at the oil/water interface of the emulsified droplets and form under further condensation an impermeable shell around the fragrant oil. The typical amount of MF resin[11] used for this encapsulation will be referred to as '100%' or 'standard amount' in the following discussion. The amount of resin was decreased from 100 to 75 to 50 and 25% to obtain microcapsules with thinner shells. All other process parameters were kept constant.

The dispersity in size of the studied microcapsules is typical for an emulsion droplet based in situ polymerization. Microcapsules with smaller average diameters show a narrower size distribution than capsules with larger average diameters.[43,44] Figure 1 presents the optical micrographs and size distributions of the produced capsules with a corresponding average diameter d for each sample size distribution summarized in Table 1. The size distributions of two additional samples produced from 100 and 50% amount of amino resin are indicated in the Table 1, but not shown in Figure 1. In particular, we observed for the produced capsules a mean diameter d_{mean} of about 30 μm. Samples that significantly deviated from this mean diameter were microcapsules produced from 75 and 25% amino resin with an average diameter of 18 and 43 μm respectively. Such variations in size are well-known and reflect the actual situation of the industrial production, which already has been reported previously.[13,44] The success and/or failure of the encapsulation process are clearly indicated in the optical micrographs in Figure 1. Spherically shaped capsules with an amino resin level of 100, 75, and 50% indicate a successful encapsulation of the oil phase. The shape of the microcapsules produced from a 25% level of amino resin was in contrast to the other batches strongly deformed. Here the encapsulation process was not successful, and the formed shell was not stable enough to encapsulate the oil phase.

To access the shell thickness of the microcapsules we used ultrathin sections of Epon-embedded microcapsules, which we analyzed with TEM. In Figure 2 examples of such sections are shown for capsules produced from different amount of amino resin. For all investigated samples, we observed a smooth shell with uniform density and rather uniform thickness. For microcapsules produced from 25% amino resin we were not able to obtain any ultrathin sections of the embedded capsules. The measured shell thickness of one section is denoted h_i and refers to an average of six analyzed cross sections, which were extracted from one TEM image. With this method, we were able to determine the shell thickness h_i with an accuracy of 12%. For each microcapsule batch, we used n number of sections to quantify the shell thickness indicated in the histograms displayed in Figure 2. From this thickness distributions we were able to determine a mean measured shell thickness h_i from the maximum of the gauss fit.

In general, we observed a decrease of h_i from 285 to 103 nm when we reduced the amount of amino resin from 100% to 50%. The observed mean shell thickness for each batch is summarized in Table 1. In Figure 2, we grouped our results according to the employed amount of amino resin and the average capsule diameter. The size distribution of the produced capsules is as important as the resin concentration for the final shell thickness of the capsules. If the volume of the dispersed phase and the resin concentration were constant, thinner shells would be expected for batches with smaller capsules compared to those with larger capsules.[13] The change in thickness is caused through an alteration of the total surface area of the dispersed phase available during the polymerization reaction, which will be larger for smaller emulsion droplets than for larger droplets. We observed this trend as well for the two samples produced from 100% amino resin, where the mean shell thickness was reduced from 285 to 215 nm, when the average diameter of the capsules decreased from 34 to 31 μm, as indicated in Figure 2. For samples whose average diameter was reproduced, as for capsules made of 50% amino resin and average diameter of 28 μm, no significant difference in the shell thickness was observed. Therefore, we combined h_i values of both batches in one diagram, shown in Figure 2.

When spherical particles are sectioned at random distance from the center, the measured diameter r_i will be smaller than the true diameter r and the measured thickness h_i will be larger than the true thickness h. On average, we obtained a standard deviation of the mean measured shell thickness of about 26%. This deviation is higher than the accuracy of the method of 12% and reflects the uncertainty of the random sectioning process. Smith and co-workers[45] introduced a correction factor accounting for the thickness artifacts produced by the random slicing process. They described the shell thickness h as a function of the slicing angle, the measured radius, and the measured shell thickness. With an estimated limit for the slicing angle about 80°, we determined the correction factor f to be about 0.62. The obtained correction factor for each batch and the corresponding corrected shell thickness h can be found in Table 1.

To estimate the available mean total surface area, a mean diameter of 30 μm, mean mass of 95 g and a density of 0.96 g/mL for the fragrance composition was used. For a constant volume of the dispersed phase, the total surface area of the emulsion droplets will decrease with increasing particle radius. In eq 1, the change of the total surface area A_{total} of microcapsules is shown when their radius is changed from r_1 to r_2. The index 1 refers to capsules characterized by the radius r_1 and index 2 to the capsule characterized by the radius r_2. A_{total} of the dispersed phase can be described by the surface area A_1 of the individual oil droplets multiplied by the number n of droplets. The number n of particles is obtained by the volume of the dispersed phase V divided by the volume of the dispersed particles V_1. With regard to the application the volume of the dispersed phase V can be easily controlled at the start of the synthesis and the mean radius of micrometer-sized capsules that is determined by the emulsion droplet size can be assessed by standard techniques for quality assurance. As eq 1 shows, the ratio of the total surface area for microcapsules with different diameters is the same like the ratio between the two capsule radii when the volume of the dispersed phase is constant

$$\frac{A_{1,total}}{A_{2,total}} = \frac{n_1 A_1}{n_2 A_2} = \frac{\frac{V}{V_1}A_1}{\frac{V}{V_2}A_2} = \frac{r_2}{r_1} \quad (1)$$

with $V_1 = V_2 = V$; $V_i = 4/3\pi r_i^3$; and $A_i = 4\pi r_i^2$, it follows that $A_i/V_i = (4\pi r_i^2)/(4/3\pi r_i^3) = 3/r_i$.

For the production of the studied capsules, the volume of the dispersed phase was constant for the different amounts of amino resin. For microcapsules that showed a deviation from the expected mean radius of 30 μm the average total surface area could be corrected by the ratio of the capsule radii, where r_1 refers to the expected mean capsule radius and r_2 to the radius of the actual produced microcapsules. Figure 3 describes

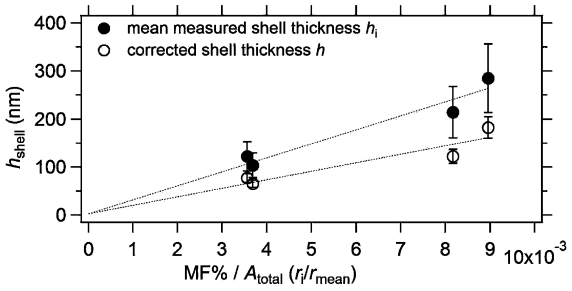

Figure 3. Shell thickness is a function of the ratio of resin amount (MF %) per total surface area of the dispersed phase. The lines were added as a guide to the eye.

the shell thickness as a function of the amount of amino resin per total surface area. Both results of the measured and the corrected shell thickness are displayed. As a trend, we can observe an increase of the shell thickness with an increase of the MF amount per total surface area, which was already reported for MF microcapsules by Sgraia et al.[13] In view of the complex nature of the manufacturing process inherent to the application-oriented study and the characterization method, the observed error margins are to be expected. We are confident that our analysis of a relatively large number of sections and the performed correction of the random sectioning process takes these variations into account. The morphological characterization and the correlation to simple and accessible process parameters showed that it is possible to adjust and predict the thickness for the investigated process. Both analysis and correlation provide strategies to realize an adjustment of the shell thickness for microcapsules produced by in situ polymerization.

Mechanical Properties. The mechanical response of immobilized microcapsules was studied by force-deformation experiments with atomic force microscopy (AFM). We used cantilevers modified with a colloidal probe to ensure an axisymmetric and uniform compression of the microcapsules. An AFM mounted on an optical microscope ensures optical control over the alignment of probe and sample. Immobilized capsules are recognized by the presence of an apparent contact area by using the microscope in microinterferometry mode.[37] In Figure 4, the typical change of the apparent contact area for an elastic response of the microcapsule is shown. The time in seconds displayed on the x-axis corresponds to the length of the video that can be found in the Supporting Information. The apparent contact area refers to the dark spot in the middle of the interference pattern, shown in the insets in Figure 4. During the first 5 s, there is no compression of the capsule and the contact area shows the immobilized capsule in uncompressed state. After 5 s, the cantilever reaches the capsule and the contact area linearly increases with further compression until the maximum deformation is reached. The cantilever retraction

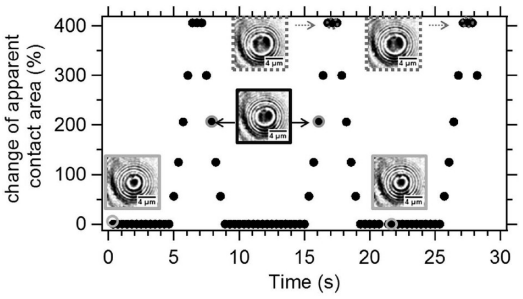

Figure 4. Uniform and elastic deformation of a microcapsule observed with an optical microscope using microinterferometry (corresponds to the video in the Supporting Information file). The investigated capsule with a diameter of 30 μm was deformed by 870 nm, corresponding to a relative deformation of 2.91%.

ends the deformation cycle and indicates the same curve progression as for the compression. The apparent contact area returns to its initial state before it is deformed again. The constant and periodic change of the apparent contact area during the presented three consecutive load−unload cycles clearly indicates a uniform and elastic compression of the capsule and the recovery of its original contact area and shape. This optical control is crucial to ensure the correct alignment between probe and sample and to carry out a reproducible capsule deformation.

To assess the mechanical properties of the shell we performed all compression experiments in the small deformation regime. For our approach as already highlighted in the introduction, the critical parameter to distinguish between small and large deformations is the shell thickness. In Figure 5A the deformation process of a thick-shelled and a thin-shelled microcapsule is illustrated. As expected for capsules with comparable size, the thin-shelled capsule deforms stronger than the thick-shelled capsule under the same force load. In this example, the thick-shelled capsules synthesized from the standard amount of amino resin show a mean shell thickness about 185 nm. The thin-shelled microcapsules were produced from 50% level of amino resin and refer to a thin shell with a thickness about 65 nm. The capsule with the thick shell deforms less than 10 nm, whereas the capsule with a thin shell deforms by 50 nm. In both cases, we observe a linear increase of the deformation with increasing force load, which represents a typical scaling behavior for a capsule deformation in the small deformation regime.[46]

The slope of the force-deformation curves reflects the compression of the capsule under the applied force load, referred to as the capsule's stiffness in units of N/m. In Figure 5B, 30 repeated force deformation cycles of the thin- and thick-shelled capsules are shown. The observed stiffness values are constant for both capsules throughout the repeated compression, illustrating that no altering of the capsules' stiffness is obtained through consecutive deformation. We also investigated the influence of fast and slow deformation rates on the microcapsules' stiffness. The used deformation rates of 10 μm/s and 0.625 μm/s did not significantly affect the mechanical response of thick-shelled microcapsules. For thin-shelled capsules, we observed an increase of the stiffness about 12% for faster deformations.

To quantify the stiffness of the capsules produced from different amount of amino resin, we measured a representative number n of aminoplast microcapsules with a slow deformation

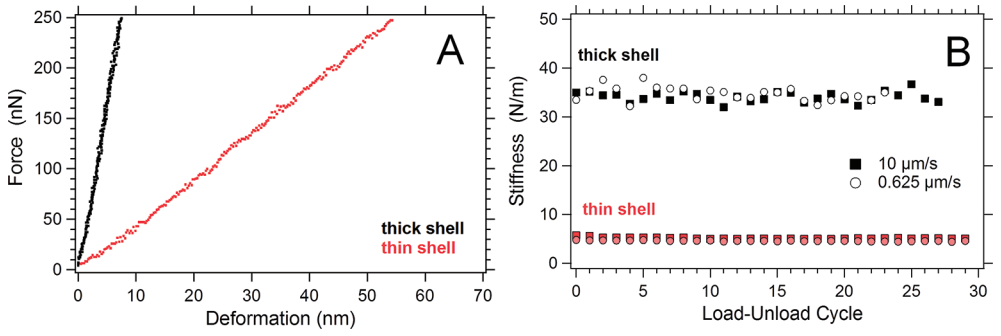

Figure 5. (A) Compression of capsules under the same force will yield larger deformations for thin-shelled capsules compared with thick-shelled capsules. (B) Microcapsules compression is elastic and the stiffness is constant over thirty load−unload cycles.

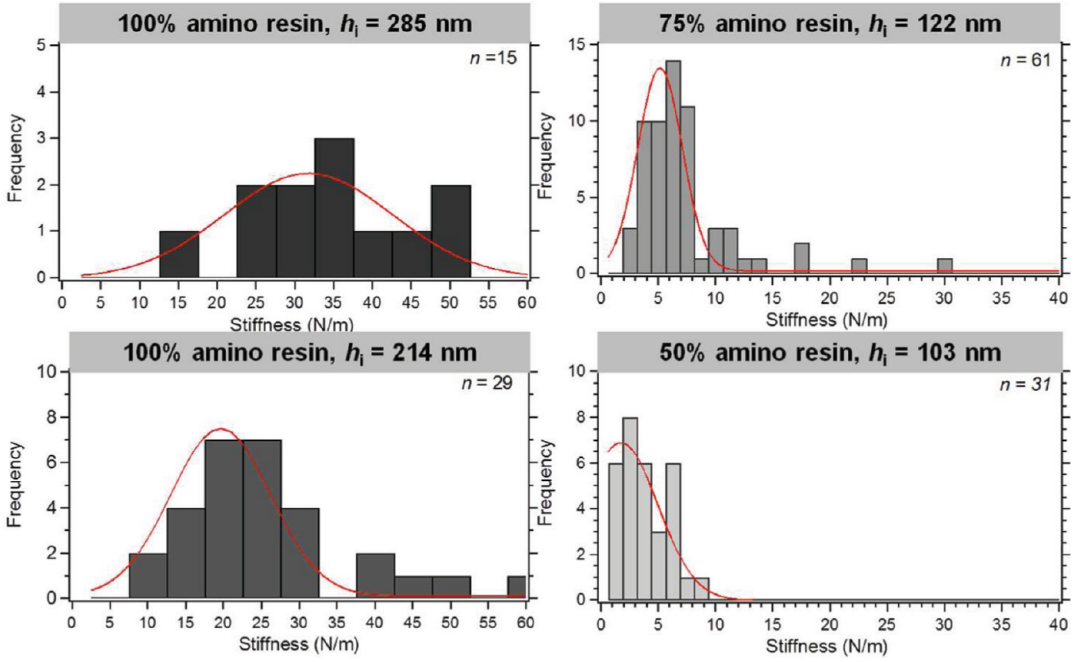

Figure 6. Capsules become softer with thinner shells, shown by the decrease of the mean stiffness for capsules with reduced shell thickness.

rate of 0.5 μm/s. In Figure 6, the distributions of the measured stiffness values present a decrease of the mean stiffness from about 30 N/m to 2 N/m for a change of the shells thickness from 285 to 103 nm, respectively. The capsules' stiffness strongly depends on the capsules' diameter. Hence, smaller microcapsules will be stiffer than larger capsules, if they were produced from the same batch and have the same shell thickness. For example, standard core/shell microcapsules with a mean shell thickness of 214 nm showed an increase in the capsule stiffness from 14 N/m to 35 N/m when the diameter of the capsule was decreased from 30 to 14 μm. Therefore, the width of the stiffness histograms is also reflecting the size distribution of the investigated capsules within one batch. The mean stiffness value determined from the histogram for each capsule batch can be found in Table 1.

In Figure 7, all results obtained from the morphological and mechanical characterization of the aminoplast capsules are displayed in relation to the used process parameters. Both shell thickness and capsule stiffness increase with the amount of amino resin per total surface area. It already has been shown[30] that properties determined in the small deformation regime play an important role for macroscopic properties such as the capsule's adhesion. In the case of MF-shelled microcapsules,

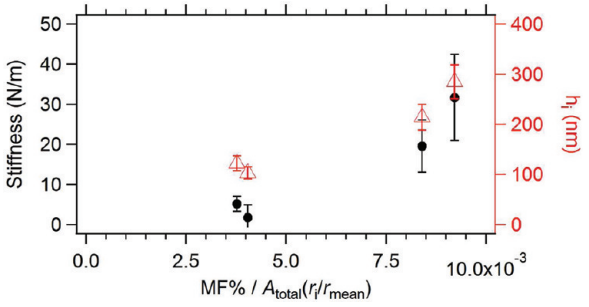

Figure 7. Summary of the morphological and mechanical characterization of aminoplast core/shell capsules and the influence of used process parameters.

with a uniform, closed, and rather strong shell, it would be interesting to link the results gained from the small deformation regime with the already well investigated rupture force of aminoplast microcapsules.[22,23]

Zhang and co-workers[23,29] showed that the deformation at burst is one of the key parameters for the rupture of aminoplast microcapsules. As discussed before the deformation behavior of microcapsules is strongly linked to the thickness of their shell,

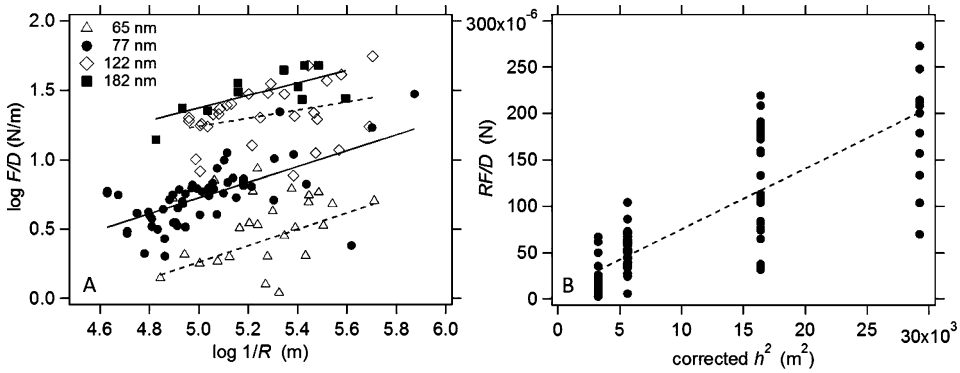

Figure 8. (A) Stiffness displayed in relation to the reciprocal radius clearly indicates an increase in the stiffness for capsules with thicker shell and comparable radius. (B) Linear relationship displayed in this graph can be correlated to the material constants of the shell material and an elastic modulus of 1.7 GPa can be estimated.

as shown in Figure 5A, where thin-shelled capsules deform much more under an applied load than thick-shelled capsules. Microcapsules burst when a critical compression is reached, which was for MF capsules reported about 70% relative deformation at burst.[36] The force loads needed for a burst will be reached for smaller force loads in the case of thin-shelled capsules compared with thick-shelled capsules. Therefore, the observed correlations present a potential strategy to be further linked with the reported macroscopic rupture forces. Such a relation would be beneficial for the tailoring of aminoplast microcapsule mechanics used in various applications with very different requirements.

The tendency observed in Figure 7 can be further analyzed to understand how the shell thickness influences the microcapsule mechanics. The mechanical response obtained from the small deformation regime can be used to understand structure property relations, because the mechanical response can be linked to the capsule's geometry and the shell's material properties.[20] According to Reissner, the measured stiffness F/D is a function of the capsules geometric parameters, radius R and the shell thickness h and the properties of the shell material, elastic modulus E and Poisson ratio ν:

$$\frac{F}{D} = \frac{h^2}{r}\frac{E}{\sqrt{3(1-\nu^2)}/4} \tag{2}$$

As described in a previous study[46] the regime valid for Reissner's prediction[47,48] of a linear scaling behavior of the applied force F with the resulting deformation D can be easily estimated based on the shell thickness h and the radius r of the capsule:

$$\varepsilon_{\text{crossover}} \approx \sqrt{\frac{h}{4\pi r}} \tag{3}$$

A critical relative deformation ε is obtained that refers to the crossover of the linear deformation regime with the deformation caused by volume forces, which scales proportional to D^3. Thus, the morphological characterization can be used to estimate the deformation regime where Reissner's prediction is valid (see Table S1 in the Supporting Information).

In Figure 8A, the measured stiffness is displayed in relation to the capsule radius. All samples show an increase in the stiffness with decreasing capsule diameter, which is in accordance with Reissner's model. The linear relation is then described by the proportionality factor, which is the square of the shell thickness and the material constants E and ν. The stiffness of microcapsules with comparable diameters increases with increasing shell thickness as Figure 8A clearly indicates. The stiffness normalized by the size plotted versus the shell thickness shows a linear relation that can be used to estimate Young's modulus of the microcapsules' shell (Figure 8B).[41,49] The Poisson ratio ν is expected to be between 0.33 for a solidlike material and 0.5 for rubber-like materials. Equation 2 describes the impact of Poisson's ratio on the resulting elastic modulus. In order to make the impact of ν transparent, we calculated the elastic modulus for both extremes. From Figure 8B, we are able to estimate the elastic modulus of the shell material of about 1.7 GPa for a Poisson ratio of 0.5, which is in good agreement with the elastic modulus reported recently by Mercadé-Prieto et al.,[29] and for a Poisson ratio 0.33 of about 2.2 GPa. However, as Figure 8B displays a certain spread of the individual data remains even after the normalization of the data by size and shell thickness. One reason for this spread can be due to differences in the shell density caused by kinetic differences during the shell formation. Salaun and co-workers[50] showed that different surface morphologies of the capsules shell are dependent on the formation of the MF precondensate. They concluded that a rather rapid shell formation will yield higher oligomers or even small MF particles in the continuous phase, which will be deposited at the oil/water interface.[32,50] The melamine to formaldehyde ratio, pH and temperature were identified as important parameters to affect the kinetics of the precondensate formation. Based on the formed oligomers, which represent the building blocks of the shell, a rougher or smoother capsule shell is obtained.[12] From this perspective and based on the results of our mechanical characterization, we think that the size of the formed oligomers and their assembly to a shell is an important aspect for shell mechanics that would be of interest for further studies.

CONCLUSION

In conclusion, we showed how mechanical properties of aminoplast microcapsules correlate with process parameters for an industrially relevant microencapsulation process, the in situ polymerization of amino resins. With the help of a thorough morphological analysis we were able to determine the microcapsule's geometric parameters, radius and shell thickness. The mechanical response of the microcapsules was investigated in form of small deformations on the order of the shell thickness, using an AFM and the colloidal probe technique. Both results, from geometrical and micromechanical character-

ization, were explained in the framework of a simple analytical model for microcapsule deformation, the Reissner shell theory. On the basis of the results, we identified the ratio of amino resin to total emulsion surface area as key parameter for controlling the microcapsules geometry and mechanical properties. Thus, a rational design of mechanical properties of aminoplast microcapsules is in reach.

■ ASSOCIATED CONTENT

Supporting Information

Additional data on the definition of the small deformation regime is available as well as a video recording the capsule deformation in situ with optical microscopy used in micro-interferometry mode. This material is available free of charge via the Internet at http://pubs.acs.org/.

■ AUTHOR INFORMATION

Corresponding Author

*Tel.: +49 921 55 2753. Fax: + 49 921 55 2059. E-mail: andreas.fery@uni-bayreuth.de.

Notes

The authors declare no competing financial interest.

■ REFERENCES

(1) Sukhorukov, G.; Fery, A.; Möhwald, H. *Prog. Polym. Sci.* **2005**, *30*, 885−897.
(2) Becker, A. L.; Johnston, A. P. R.; Caruso, F. *Small* **2010**, *6*, 1836−1852.
(3) Nelson, G. *Int. J. Pharm.* **2002**, *242*, 55−62.
(4) Madene, A.; Jacquot, M.; Scher, J.; Desobry, S. *Int. J. Food Sci. Technol.* **2006**, *41*, 1−21.
(5) Jacquemond, M.; Jeckelmann, N.; Ouali, L.; Haefliger, O. P. *J. Appl. Polym. Sci.* **2009**, *114*, 3074−3080.
(6) Rokka, S.; Rantamaki, P. *Eur. Food Res. Technol.* **2010**, *231*, 1−12.
(7) Sanchez, L.; Lacasa, E.; Carmona, M.; Rodriguez, J. F.; Sanchez, P. *Ind. Eng. Chem. Res.* **2008**, *47*, 9783−9790.
(8) Mauldin, T. C.; Kessler, M. R. *Int. Mater. Rev.* **2010**, *55*, 317−346.
(9) Quellet, C.; Schudel, M.; Ringgenberg, R. *Chimia* **2001**, *55*, 421−428.
(10) Dietrich, K.; Herma, H.; Nastke, R.; Bonatz, E.; Teige, W. *Acta Polym.* **1989**, *40*, 243−251.
(11) Haefliger, O. P.; Jeckelmann, N.; Ouali, L.; Leòn, G. *Anal. Chem.* **2010**, *82*, 729−737.
(12) Lee, H. Y.; Lee, S. J.; Cheong, I. W.; Kim, J. H. *J. Microencapsul.* **2002**, *19*, 559−569.
(13) Sgraja, M.; Blömer, J.; Bertling, J.; Jansens, P. J. *J. Appl. Polym. Sci.* **2008**, *110*, 2366−2373.
(14) Su, J.-F.; Wang, L.-X.; Ren, L.; Huang, Z. *J. Appl. Polym. Sci.* **2007**, *103*, 1295−1302.
(15) Yuan, Y. C.; Rong, M. Z.; Zhang, M. Q. *Polymer* **2008**, *49*, 2531−2541.
(16) Balazs, A. C. *Mater. Today* **2007**, *10*, 18−23.
(17) Sliwka, W. *Angew. Chem., Int. Ed.* **1975**, *14*, 539−550.
(18) Roitman, D. B. Microcapsule Biosensors and Methods of Using the Same. US Patent 07312040, Dec 26, 2007.
(19) Esser-Kahn, A. P.; Odom, S. A.; Sottos, N. R.; White, S. R.; Moore, J. S. *Macromolecules* **2011**, *44*, 5539−5553.
(20) Fery, A.; Weinkamer, R. *Polymer* **2007**, *48*, 7221−7235.
(21) Chen, P. W.; Erb, R. M.; Studart, A. R. *Langmuir* **2011**, *28*, 144−152.
(22) Keller, M. W.; Sottos, N. R. *Exp. Mech.* **2006**, *46*, 725−733.
(23) Zhang, Z.; Saunders, R.; Thomas, C. R. *J. Microencapsul.* **1999**, *16*, 117−124.
(24) Hu, J. F.; Chen, H. Q.; Zhang, Z. B. *Mater. Chem. Phys.* **2009**, *118*, 63−70.
(25) Long, Y.; York, D.; Zhang, Z. B.; Preece, J. A. *J. Mater. Chem.* **2009**, *19*, 6882−6887.
(26) Sun, G.; Zhang, Z. *J. Microencapsul.* **2001**, *18*, 593−602.
(27) Yang, J.; Keller, M. W.; Moore, J. S.; White, S. R.; Sottos, N. R. *Macromolecules* **2008**, *41*, 9650−9655.
(28) Caruso, M. M.; Blaiszik, B. J.; Jin, H. H.; Schelkopf, S. R.; Stradley, D. S.; Sottos, N. R.; White, S. R.; Moore, J. S. *ACS Appl. Mater. Interfaces* **2010**, *2*, 1195−1199.
(29) Mercade-Prieto, R.; Nguyen, B.; Allen, R.; York, D.; Preece, J. A.; Goodwin, T. E.; Zhang, Z. B. *Chem. Eng. Sci.* **2011**, *66*, 2042−2049.
(30) Elsner, N.; Dubreuil, F.; Fery, A. *Phys. Rev. E* **2004**, *69*, 031802.
(31) Arshady, R.; George, M. H. *Polym. Eng. Sci.* **1993**, *33*, 865−876.
(32) Dietrich, K.; Bonatz, E.; Geistlinger, H.; Herma, H.; Nastke, R.; Purz, H. J.; Schlawne, M.; Teige, W. *Acta Polym.* **1989**, *40*, 325−331.
(33) Hong, K.; Park, S. *Mater. Chem. Phys.* **1999**, *58*, 128−131.
(34) Alic, B.; Sebenik, U.; Krajnc, M. *J. Appl. Polym. Sci.* **2010**, *119*, 3687−3695.
(35) Yuan, L.; Liang, G. Z.; Xie, J. Q.; Li, L.; Guo, J. *Polymer* **2006**, *47*, 5338−5349.
(36) Sun, G.; Zhang, Z. *Int. J. Pharm.* **2002**, *242*, 307−311.
(37) Dubreuil, F.; Elsner, N.; Fery, A. *Eur Phys J E* **2003**, *12*, 215−221.
(38) Butt, H. J. *Biophys. J.* **1991**, *60*, 1438−1444.
(39) Ducker, W. A.; Senden, T. J.; Pashley, R. M. *Nature* **1991**, *353*, 239−241.
(40) Hutter, J. L.; Bechhoefer, J. *Rev. Sci. Instrum.* **1993**, *64*, 1868−1873.
(41) Elsner, N.; Dubreuil, F.; Weinkamer, R.; Fischer, F. D.; Wasicek, F.; Fery, A. *Prog. Coll. Polym. Sci.* **2006**, *132*, 117−132.
(42) Butt, H. J.; Cappella, B.; Kappl, M. *Surf. Sci. Rep.* **2005**, *59*, 1−152.
(43) Yuan, L.; Gu, A.; Liang, G. *Mater. Chem. Phys.* **2008**, *110*, 417−425.
(44) Wang, H.; Yuan, Y.; Rong, M.; Zhang, M. *Colloid Polym. Sci.* **2009**, *287*, 1089−1097.
(45) Smith, A. E.; Zhang, Z.; Thomas, C. R. *Chem. Eng. Sci.* **2000**, *55*, 2031−2041.
(46) Fery, A.; Dubreuil, F.; Möhwald, H. *New J Phys* **2004**, *6*, 18.
(47) Reissner, E. *J. Math. Phys.(Cambridge, Mass.)* **1946**, *25*, 279−300.
(48) Reissner, E. *J. Math. Phys.(Cambridge, Mass.)* **1946**, *25*, 80−85.
(49) Zoldesi, C. I.; Ivanovska, I. L.; Quilliet, C.; Wuite, G. J. L.; Imhof, A. *Phys. Rev. E* **2008**, *78*, 8.
(50) Salaun, F.; Vroman, I. *Eur. Polym. J.* **2008**, *44*, 849−860.